Double-Aging Method for Preparation of Stabilized Na−Buserite and Transformations to Todorokites Incorporated with Various Metals

Jian Luo,[†] Qiuhua Zhang,[‡] Aimin Huang,[†] Oscar Giraldo,[‡] and Steven L. Suib*,[†,‡]

Department of Chemistry (U-60) and Department of Chemical Engineering and Institute of Materials Science, University of Connecticut, Storrs, Connecticut 06269-4060

Received June 17, 1998

A double-aging method has been developed to prepare and stabilize Na−buserite. In the first step, Na−buserite is synthesized by aging a MnO_x gel, which is produced from the oxidation of $Mn(OH)_2$ in NaOH solutions by $KMnO_4$ in the presence of Mg^{2+}. Stabilization of Na−buserite is done by further aging the as-synthesized buserite in distilled deionized water. Physical and chemical changes during the second aging (stabilization) have been investigated by using X-ray diffraction (XRD), infrared (IR), scanning electronic microscopy and energy-dispersive X-ray studies (SEM/EDX), thermogravimetric analysis (TGA), differential scanning calorimetry (DSC), cyclic voltammetry (CV), and temperature-programmed desorption combined with mass spectrometer (TPD-MS). The amount and type of metals incorporated into buserite and todorokite are greatly increased by the second aging treatment (including many lanthanides, whose incorporation has not been reported before). The metal species introduced in the layers considerably change the interlayer distances and, accordingly, the cell parameters. A criterion is obtained for the transformation of todorokite-type tunnel MnO_x materials from buserite-type layered MnO_x by hydrothermal treatment: only buserites which are stable at elevated temperatures in aqueous systems can convert to a todorokite structure; unstable buserites form a structure whose main *d* spacings are at 3.56 and 7.1 Å. Interconversions among several layered MnO_x are also discussed.

Introduction

Buserite and birnessite are both important manganese-containing phases in marine nodules and in some terrestrial regions.[1−9] Buserite has double layers of hydrates while birnessite has only a monolayer of hydrates (Figure 1). These layered materials are important precursors to certain one-dimensional molecular sieves, such as todorokite (OMS-1, with channels of 3 × 3 MnO_6 units),[11−13,16,17] cryptomelane (OMS-2, 2 × 2),[13,29,31] and pyrolusite (1 × 1).[26,32] The conversions among buserite, birnessite, and todorokite and their ion-exchange properties are very important topics in geochemistry and marine chemistry and may be important in the evolution of manganese oxides and the enrichment of other metals in manganese nodules.[10−13] In addition, they have found wide use as ion-exchange materials,[13−17] battery materials,[18−21] and oxidation−reduction catalysts.[10,16,17,22−26]

Buserites have herein been classified into stable buserites (stable at least at room temperature) and unstable buserites. Na−

---

[*] To whom correspondence should be addressed.

[†] Department of Chemistry.

[‡] Department of Chemical Engineering and Institute of Materials Science.

(1) Jones, L. H. P.; Milne, A. A. *Mineral. Mag.* **1956**, *31*, 283−288.
(2) Burns, R. G.; Burns, V. M. *Philos. Trans. R. Soc. London, Ser. A* **1977**, *286*, 283−301.
(3) Bricker, O. *Am. Mineral.* **1965**, *50*, 1296−1354.
(4) Giovanoli, R.; Burki, P. *Chinimia* **1975**, *29*, 266−269.
(5) Turner, S.; Buseck, P. R. *Science* **1979**, *203*, 456−458.
(6) Turner, S.; Buseck, P. R. *Science* **1981**, *212*, 1024−1027.
(7) Siegel, M. D.; Turner, S. *Science* **1983**, *219*, 172−174.
(8) Taylor, R. M.; Mckenzie, R. M.; Norrish, K. *Aust. J. Soil Res*. **1964**, *2*, 235−248.
(9) Chukhrov, F. V.; Gorshkov, A. I. *Trans. R. Soc. of Edinburgh* **1981**, *72*, 195−200.
(10) Wong, S. T.; Cheng, S. *Inorg. Chem*. **1992**, *31*, 1165−1172.
(11) Golden, D. C.; Chen, C. C.; Dixon, J. B. *Clays Clay Miner*. **1987**, *35*, 271−280.
(12) Golden, D. C.; Chen, C. C.; Dixon, J. B. *Science* **1986**, *231*, 717−719.
(13) Golden, D. C.; Dixon, J. B.; Chen, C. C. *Clays Clay Miner*. **1986**, *34*, 511−520.
(14) Straczek, J. R.; Horen, A.; Warshaw, C. M. *Am. Mineral*. **1960**, *45*, 1174−1184.
(15) Burns, R. G.; Burns, V. M.; Stockman, H. *Am. Mineral*. **1983**, *68*, 972−980.
(16) Shen, Y. F.; Zerger, R. P.; DeGuzman, R. N.; Suib, S. L.; McCurdy, L.; Potter, D. I.; O'Young, C. L. *J. Chem. Soc., Chem. Commun.* **1992**, 1213−1214.
(17) Shen, Y. F.; Zerger, R. P.; DeGuzman, R. N.; Suib, S. L.; McCurdy, L.; Potter, D. I.; O'Young, C. L. *Science* **1993**, *260*, 511−515.
(18) Pereira-Ramos, J. P.; Badour, R.; Bach, S.; Baffier, N. *Solid State Ionics* **1992**, *701*, 3−56.
(19) Bach, S.; Pereira-Ramos, J. P.; Baffier, N. *Electrochim. Acta* **1993**, *38*, 1695−1700.
(20) Bach, S.; Pereira-Ramos, J. P.; Baffier, N. *J. Solid State Chem*. **1995**, *120*, 70−73.
(21) Ruetschi, P. J.; Giovanoli, R. *J. Electrochem. Soc.* **1988**, *135*, 2663−2669.
(22) Jiang, S. P.; Ashton, W. R.; Tseung, A. C. C. *J. Catal*. **1991**, *131*, 88−94.
(23) Nitta, M. *Appl. Catal.* **1984**, *19*, 151−176.
(24) Yin, Y. G.; Xu, W. Q.; Shen, Y. F.; Suib, L. S. *Chem. Mater*. **1994**, *6*, 1803−1808.
(25) O'Young, C. L.; Shen, Y. F.; Zerger, R. P.; Suib, S. L. U.S. Patent 5340562, 1994.
(26) Shen, Y. F.; Suib, S. L.; O'Young, C. L. *J. Catal*. **1996**, *161*, 115−122.
(27) Luo, J.; Segal, S. R.; Wang, J. Y.; Tian, Z. R. *Proc. Mater. Res. Soc., San Francisco* **1996**, 3−8.
(28) Luo, J.; Suib, S. L. *J. Chem. Soc., Chem. Commun*. **1997**, 1031−1032.
(29) Chen, C. C.; Golden, D. C.; Dixon, J. B. *Clays Clay Miner*. **1986**, *34*, 565−571.
(30) Giovanoli, R.; Balmer, B. *Chinimia* **1981**, *35*, 53−55.
(31) Giovanoli, R.; Faller, M. *Chinimia* **1989**, *43*, 54−56.
(32) Feng, Q.; Kanoh, H.; Miyai, Y.; Ooi, K. *Chem. Commun.* **1996**, 1607−1608.

10.1021/ic980675r CCC: $18.00

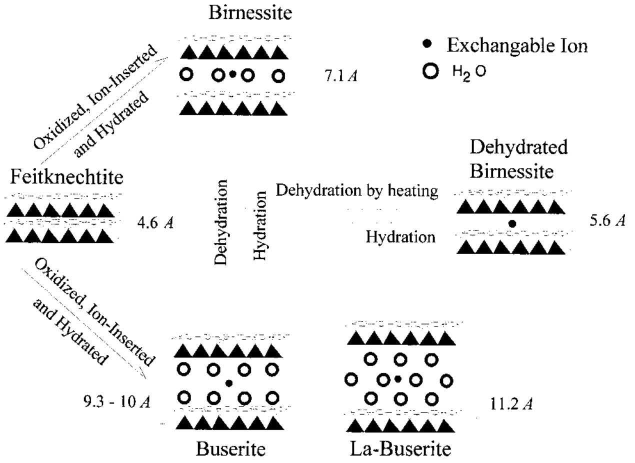

Figure 1. Conversions Among Feitknechtite, Buserite, Birnessite, and Dehydrated Birnessite.

buserite prepared by previous methods is unstable, very easily losing a part of the hydrates to form Na−birnessite at room temperature in air.[11,13,33,34] This makes studies of Na−buserite very difficult. For example, in IR studies of Na−buserite some painstaking procedures are necessary to protect buserite from changing to birnessite.[33] As a result, the preparation of Na−buserite that is stable at least at room temperature and under common humidity conditions is useful for facile characterization of Na−buserite.

The preparation of metal-doped todorokites, which are generally synthesized from hydrothermal treatment of metal−buserites, has been the subject of several studies due to their promising catalytic properties.[35−37] Few stable buserites are known. So far, only a few group II or transition metal ions have been incorporated into unstable Na−buserite, such as Mg^{2+}, Cu^{2+}, Zn^{2+}, Ni^{2+}, Co^{2+}, and Mn^{2+}. As a result, the number of metals incorporated into todorokite from these metal−buserite precursors is limited.

In this work, a procedure for the formation and stabilization of Na−buserite has been reported. Comparisons have been made among stabilized Na−buserite, unstable Na−birnessite, and Mg−buserite in aspects such as hydrate-retaining ability, framework thermal stability, morphology, and IR framework vibrational behavior. The transformation from metal−buserite type layered MnO_x to tunnel MnO_x has been investigated. The number of metals incorporated into todorokite is greatly increased via double-aged buserite. These metals include most group I/II metals, many more transition metals, and many lanthanides. On the basis of these results, a criterion for the formation of metal-incorporated todorokites has been obtained.

Experimental Section

A. Preparation of Na−Buserite. Syntheses of Na−buserite were mainly done via synthesis I as follows: A solution of 19.6 g of $MnAc_2 \cdot 4H_2O$ and 3.4 g of $MgAc_2 \cdot 4H_2O$ in 140 mL of distilled deionized water (DDW) was added slowly to a solution of 50 g of NaOH in 160 mL of DDW under vigorous stirring, forming a white slurry of $Mn(OH)_2$. A solution of 4.8 g of $KMnO_4$ in 140 mL of DDW was added slowly to the slurry under vigorous stirring, producing a brownish black suspension of MnO_x. The suspension was aged statically at 40 °C for 1−4 days. For the preparation of uniform large-size (ca. 10 μm) Na−buserite, the synthesis was done at room temperature for 15 days with 85 g of NaOH (synthesis II). Similar procedures have been reported in our previous work.[36]

B. Stabilization of Na−Buserite. Well-crystallized product was filtered out and washed until the pH of the filtered solution was below 9.5. A part of the washed sample was dried at room temperature for studies of unstable Na−birnessite. The rest of the product was transferred to a 1000 mL beaker with 800 mL of DDW under mild stirring for 2 days. The product was then filtered out. A part of the cake was dried in air at room temperature to prepare stabilized buserite for the characterization studies. The rest of the wet product was used for ion-exchange.

C. Ion-Exchange of Na−Buserite and Subsequent Conversion to Todorokites. A 200 mL solution of various metal salts with normal hydrates (0.2−0.5 mol/L, the salt anions can be nitrate, acetate, or chloride) was used for ion exchange. About 2 mL of Na−buserite (either stabilized or unstable, while still wet) was added into the salt solution with mild stirring for about 10 h at room temperature. Solutions of 1 mol/L of chlorides of Mg^{2+}, Cu^{2+}, Ni^{2+}, Co^{2+}, Zn^{2+}, and Mn^{2+} were also used for ion exchange.

An exchanged metal−buserite was filtered and transferred to a 100 mL Teflon-lined autoclave. For the preparation of main-group-metal todorokites, DDW was added to make the autoclave approximately $^3/_4$ full. For the preparation of other metal−todorokites, solutions of 0.1 M of their salts were used to fill the autoclave ca. $^3/_4$ full. The autoclaves were heated statically at 150 °C for 2 days. The products were metal−todorokites.

D. Characterization by XRD, SEM, IR, TGA/DSC, CV, and TPD-MS. X-ray diffraction experiments were done on a Scintag XDS 2000 X-ray diffractometer using a tube voltage of 45 kV and a tube current of 40 mA with Cu Kα radiation. For each determination, 10 drops of the sample slurry were placed on the sample glass slide. When dried in air, the sample formed a uniform thin film on the slide. A wet sample is dark black while a dried sample is grayish. A color change is observed when the sample film is dried.

SEM photographs of the samples were taken on an AMRAY 1810 D scanning electronic microscope. The voltage used for both SEM studies and EDX studies was 20 kV. The IR experiments were done on a Nicolet Magna-IR System 750 FT-IR spectrometer using standard procedures of single-beam diffuse reflectance methods with an MCT-B detector and a KBr beam splitter. For each sample, 200 scans were taken with a resolution of 4 cm^{-1}.

TGA profiles were made on a Hi-Res TGA 2950 thermogravimetric analyzer (TA instruments). DSC experiments were carried out on a DSC 2900 differential scanning calorimeter (TA instruments). The samples were heated in N_2 from room temperature to required temperatures at a rate of 10 °C/min and held at the final temperatures for 10 min. In separate analyses, the temperature was held at 200 °C for 30 min to determine the water content.

CV studies were done at pH = 4. Samples were made as described in ref 37. For TPD-MS experiments, 0.10 g of a sample (after preabsorption of CO_2 in air) was loaded into a U-type quartz tube placed in a temperature-programmed furnace. No heating pretreatment was done because the sample might undergo dehydration. After the sample was purged in helium for 1 h, the temperature was increased at 10 °C/min to 750 °C. The down stream gas was detected by a quadrupole MKI MS system.

Results

A. Double-Aging Method and Stabilization of Na−Buserite. Birnessites were well crystallized in ca. 2 days. When the product was not fully dried, the product was Na−buserite. When fully dried, the product existed as birnessite. Figure 2c shows the XRD pattern of an intermediate converting buserite to birnessite. The conversion was reversible at room temperature. When the converted Na−birnessite was stirred in water, it

---

(33) Potter, R. M.; Rossman, G. R. *Am. Mineral*. **1979**, *64*, 1199−1218.

(34) Tejedor-Tejedor, M. I.; Paterson, E. *Proc. Int. Clay Conf.* **1978**, 501−508.

(35) Shen, Y. F.; DeGuzman, R. N.; Zerger, R. P.; Suib, S. L.; O′Young, C. L. *J. Am. Chem. Soc*. **1994**, *116*, 11020−11029.

(36) **(**36**)** Luo, J.; Suib, S. L. *J. Phys. Chem. B* **1997**, *101*, 10403−10413.

(37) DeGuzman, R. N.; Shen, Y. F.; Suib, S. L.; Shaw, B. R.; O′Young, C. L. *Chem. Mater*. **1993**, *5*, 1395−1400.

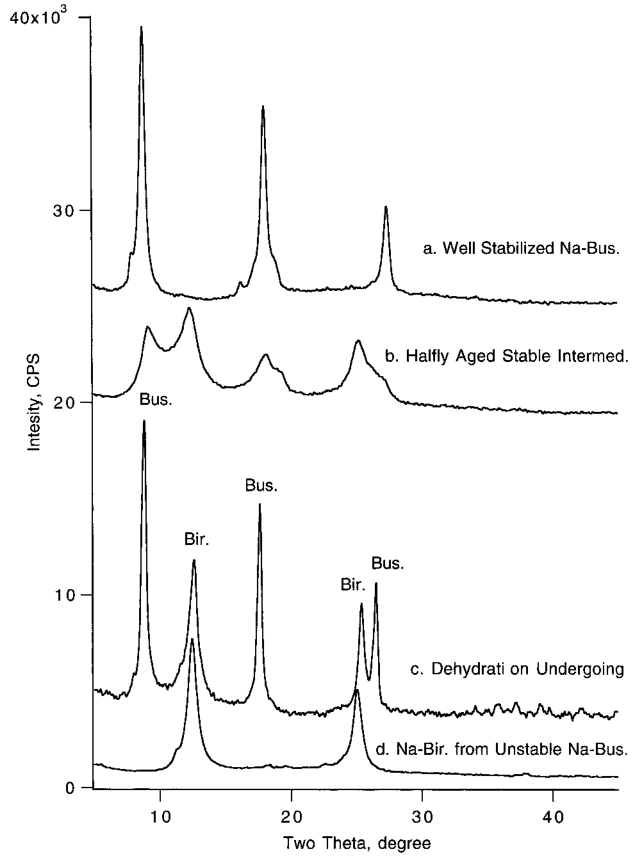

Figure 2. XRD Patterns of Well-Aged Stabilized Na−Buserite (a), Stable Intermediate (b), Unstable Intermediate Changing from Buserite to Birnessite (c), and Na−Birnessite (d).

changed back to Na−buserite. The conversion became partially irreversible over 65 °C.

The double-aged sample had a buserite structure and retained this structure after the sample had been exposed in air (relative humidities are usually 21−34%) at room temperature for 6 months (Figure 2a). The structure did not change even after it was heated at 40 °C for 30 min. This resulted in a stabilized Na−buserite. The procedure contained two aging processes and was therefore called double aging.

Stabilized Na−buserite gradually changed to Na−birnessite when the sample was heated over 50 °C. The converted sample can also change back to buserite when it was stirred in water for 30 min. Unlike untreated Na−buserite, the conversion for stabilized Na−buserite was still reversible even when it was heated to 65 °C for 30 min but was only partially reversible when it was heated at 80 °C for 30 min even though it was stirred in water overnight.

Figure 2b shows the XRD pattern of a dried sample which was aged for only 5 h. The dried sample had characteristic peaks of both buserite and birnessite and also had continuous reflections between the corresponding peaks. Unlike the short-lived intermediate of unstable Na−buserite (Figure 2c), this incompletely aged sample (intermediate) was stable at room temperature. When heated to 40 °C for 30 min, it changed to birnessite.

B. Characterization of Stabilized Na−Buserite. Figure 3 shows the IR spectra of Na−birnessite, stabilized Na−buserite, and Mg−buserite. All three samples had similar spectra. The IR absorption around 460 and 510 cm^{-1} were diagnostic of the birnessite structure. The complex broad absorptions around 3200 cm^{-1} were due to the absorption of interlayer hydrates and from hydroxyl groups which may not be due to hydrates. The complexity of the absorptions indicated a multiplicity of water molecules and hydroxyl groups. The relatively simple absorption in the bending vibration region of water (ca. 1600 cm^{-1}) for stabilized Na−buserite with respect to unstable buserite (Na−birnessite) indicated that the ordering of hydrates in buserite was improved upon a second aging. The single peak for Mg−buserite in this region showed that the ordering became almost uniform upon Mg^{2+} exchange.

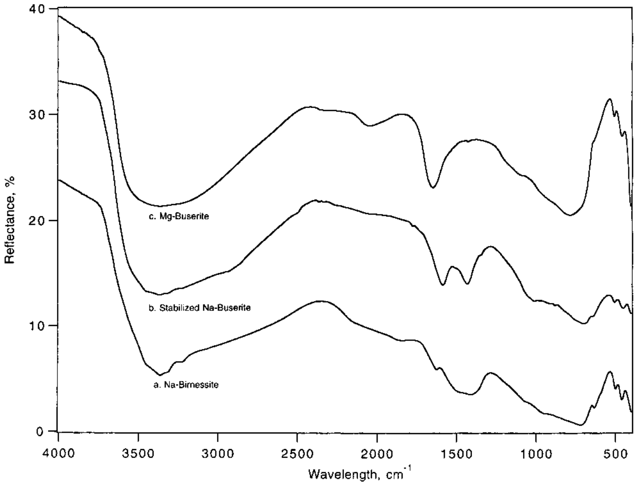

Figure 3. IR Spectra of Stabilized Na−Buserite, Na−Birnessite, and Mg−Buserite.

A Na−birnessite prepared from synthesis I consisted of flowerlike sheet aggregates. The corresponding stabilized Na−buserite and Mg−buserite had similar morphologies. Synthesis II had been employed to prepare large-size unstable Na−birnessite (Figure 4). Stabilized Na−buserite and Mg−buserite from this large-size Na−birnessite had identical hexagonal platy morphologies, indicating no morphology change during the stabilization and ion exchange of Na−buserite.

Na−birnessite, either from unstable Na−buserite or from stabilized Na−buserite, underwent a second dehydration when it was heated over 120 °C. XRD peaks corresponding to the new phase were at 5.6 and 2.8 Å. This new phase is referred to as dehydrated birnessite.[36] When heated over 400 °C, birnessite was converted into Mn_2O_3.

An endothermic peak around 140 °C with a shoulder at ca. 70 °C and a large endothermic peak at ca. 280 °C were observed in the DSC curve of an Na−birnessite. The peak around 140 °C may be due to the dehydration of Na−birnessite. The small shoulder may be from the evaporation of physisorbed water. The 280 °C peaks may be due to the decomposition of birnessite. The DSC curve of stabilized Na−buserite (Figure 5b) was similar to that of Na−birnessite, except that the shoulder had a larger area, corresponding to more adsorbed water and/or the partial dehydration of buserite to birnessite. The higher temperature peak was also around 280 °C. Mg−buserite had a dehydration peak at 170 °C. This is in accordance with the fact that the starting temperature of dehydration of Mg−buserite is higher than that of Na−birnessite. However, the high-temperature peaks for materials were all around 280 °C.

Similar results were obtained from TGA studies (Figure 5a). Stable Na−buserite, Na−birnessite, and Mg−buserite all had weight losses around 300 °C and over 500 °C. Static heating monitored by MS showed that water could be completely removed by heating at 200 °C for 30 min. Higher temperatures lead to considerable evolution of O_2. XRD shows that the products after the TGA studies were all hausmannite (γ-Mn_3O_4).

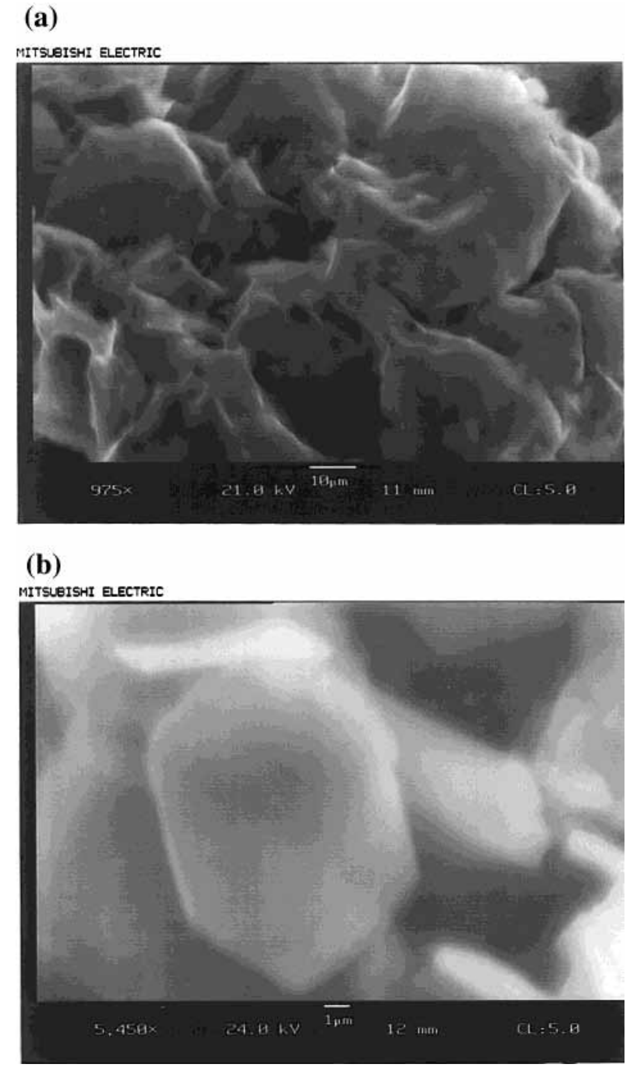

Figure 4. SEM Photographs of Stabilized Na−Buserite From Synthesis I (a) and II (b).

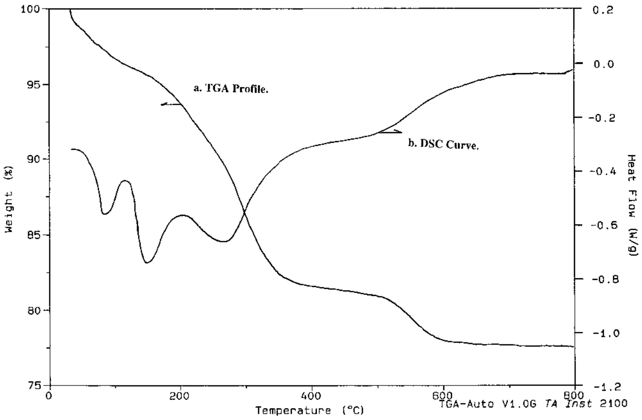

Figure 5. DSC Curve (a) and TGA Profile (b) of Stabilized Na−Buserite.

Three CO_2 peaks ($m/z = 44$), with peak temperatures at 120, 200−300, and > 400 °C, were observed in TPD-MS (Figure 6). These peaks were referred to as α (low temperature), β (medium temperature), and γ (high temperature) species of CO_2, respectively, and may correspond to CO_2 species adsorbed in different sites. Notice that the peak temperatures for both unstable and stabilized Na−buserite were similar but stabilized buserite had a smaller β-peak area. This suggests that double aging did not change the strength of basicity but decreased the density of basic sites of medium strength. Oxygen peaks ($m/z = 32$) were observed at ca. 250 and 580 °C, possibly corresponding to the decomposition of birnessite to Mn_2O_3 and Mn_3O_4, respectively.

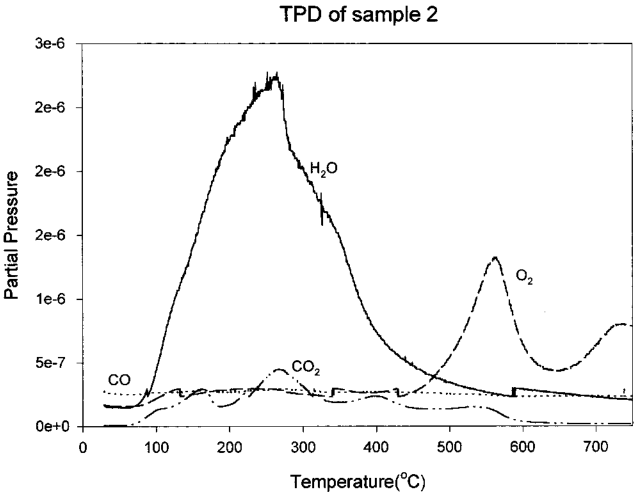

Figure 6. TPD-MS profiles of stabilized Na−buserite.

Due to the complexity of Mn in buserite/todorokite materials, XPS is not suitable to study the oxidation states of Mn in these manganese oxides. CV may provide an alternative approach. The three peaks at 0.8, 0.4, and −0.1 V may correspond to reduction of Mn^{4+}, Mn^{3+}, and Mn^{2+}.[17] Unstable Na−buserite exhibited the first two peaks while the 0.8 and −0.1 V peaks were present in the voltammogram of stabilized Na−buserite (Figure 7). This result suggests that Mn^{3+} in Na−buserite may disproportionate into Mn^{4+} and Mn^{2+} during the stabilization process.

C. Conversion of Stabilized Na−Buserite to Metal-Incorporated Todorokite. 1. Ion-Exchange of Various Metals into Unstable Na−Buserite and Phase Transformation by Hydrothermal Treatment. The ion exchange of unstable buserite with $MgCl_2$ (0.2−1 M) was very quick, being complete in less than 5 min. The resultant Mg−buserite was stable even when it was heated at 140 °C for 30 min. The ion exchange of unstable Na−buserite with Cu^{2+}, Ni^{2+}, Co^{2+}, Zn^{2+}, and Mn^{2+} also led to the formation of stable buserites, although they were less thermally stable than Mg−buserite. These buserites can be autoclaved to form M−todorokites. These results are similar to those reported by Shen et al.[35] and Golden et al.[11,13]

Figure 8 shows the XRD patterns of samples produced by ion exchange of unstable Na−buserite with group II elements (Mg, Ca, Sr, Ba) and corresponding autoclaved products. Only stable Mg−buserite was obtained. The ion exchange of Ba^{2+} produced an unstable buserite structure, changing to birnessite when it was dried (Figure 8c). The Ca^{2+}- and Sr^{2+}-exchanged samples can retain the buserite structure for 10 min to 1 h after they were dried but gradually partially changed to birnessite. Among these samples only Mg−buserite can be converted to Mg−todorokite (with XRD peaks at 9.8, 4.9, and 3.3 Å, called OMS-1) by hydrothermal treatment. The other three (Ca, Sr, and Ba) formed a structure with *d* spacing at 7.1 and 3.56 Å (called OMS-1′, Figure 8d). Some dehydrated birnessite can be observed for an autoclaved Ba−birnessite sample (Figure 8e). When unstable Na−buserite was ion-exchanged with alkali metals A (A = Li, K, Rb, Cs), only unstable A−buserites can be obtained. Hydrothermal treatments of the unstable A−bu-

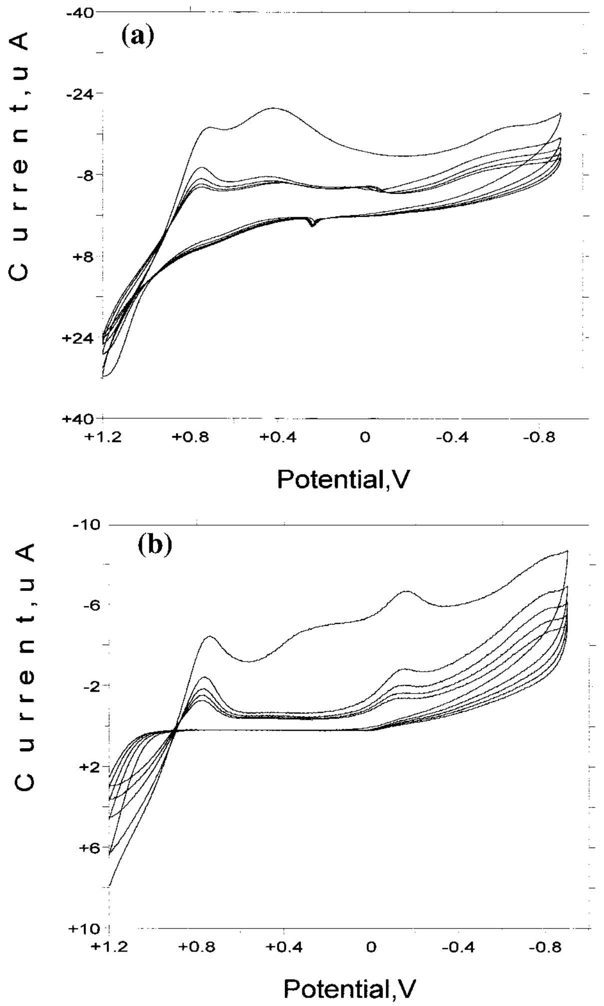

Figure 7. Cyclic Voltammograms of Na−birnessite and stabilized Na−bBuserite.

serites also led to the formation of the OMS-1′ phase. This phase is probably a variety of hollandite-type manganese oxides.[39]

2. Ion Exchange of Stabilized Na−Buserite and Conversion to Metal−Todorokite. The ion exchange of stabilized Na−buserite with Mg^{2+} was also fast (finished in a few minutes). Figure 9 shows the XRD patterns of buserites from ion exchange of stabilized Na−buserite with group II elements and corresponding autoclaved products. Stable buserites of Mg^{2+}, Ca^{2+}, and Sr^{2+} can be obtained from stabilized Na−buserite. Hydrothermal treatment of these materials can lead to the formation of the todorokite structure. Even Ba^{2+} exchange can produce an intermediate between birnessite and buserite, hydrothermal treatment of which resulted in a product intermediate between OMS-1 and OMS-1′ (Figure 9b,e). The basal *d* spacings for Mg−, Ca−, Sr−, and Ba−buserites are 9.60, 9.98, 9.47, and 7.76 Å, respectively.

Various other metals had been chosen for ion exchange, including all alkali metals other than Fr^+, all the first-row transition metals, some second-row transition metals such as Pd^{2+} and Ag^+, all the lanthanides except Sc^{3+}, Tm^{3+}, and Yb^{3+}, and some main group metals such as Al^{3+} and Sn^{2+}. Almost all of these metals (except Ba^{2+}, Cr^{3+}, and Ce^{3+}) can lead to the formation of stable metal−buserite by ion exchange. Some XRD patterns of the metal−buserites are given in Figures 10 and 12a. They are all of a buserite XRD pattern, although with some difference in *d* spacing of the basal reflection (11.2−9.3 Å). Hydrothermal treatment of these stable buserites usually led to todorokites (Figure 11) incorporated with these metals (except La^{3+}; see Figure 12a). To our knowledge, the incorporation of lanthanides other than La^{3+} into birnessites, buserites, or todorokites has not been reported.

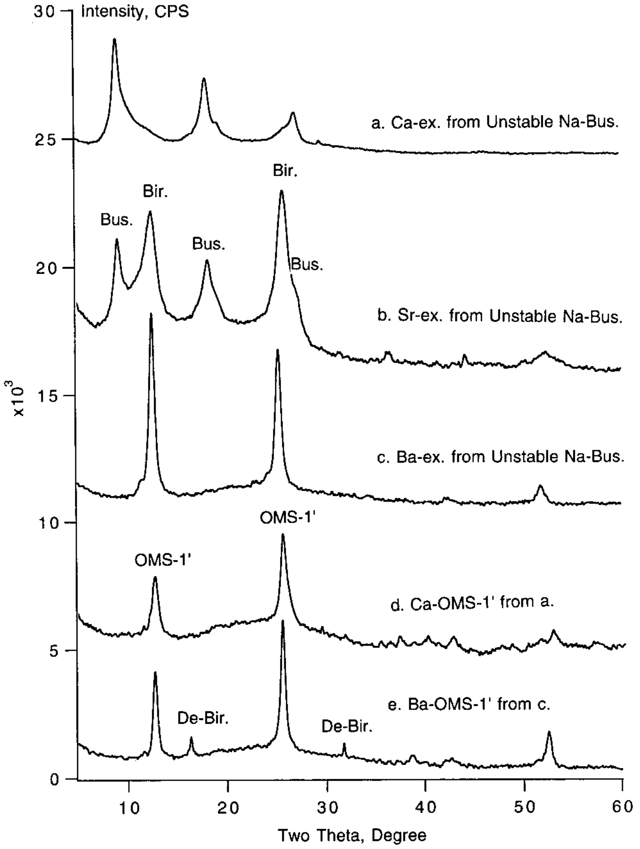

Figure 8. XRD patterns of buserites from ion exchange of unstable Na−buserite with group II metals and corresponding autoclaved products (150 °C for 2 days).

Some exceptions were the ion exchange of stabilized Na−buserite with Ba^{2+}, Ce^{3+}, and Cr^{3+}. The ion-exchanged products were unstable buserites, having typical buserite-type XRD patterns when they were wet or newly dried. When dried in air, they all had very broad, irregular XRD peaks at a position between those of the corresponding buserite and birnessite phases. Hydrothermal treatment of these materials led to an almost amorphous product or a product with some extremely broad XRD reflections (see Figures 9 and 12).

The compositions of Na−birnessite (without stabilization), Na−buserite (stabilized), and some metal−buserites from Na−buserite exchanged with various metal ions are listed in Table 1. The content of Na^+ decreased considerably after stabilization. After Na−buserite was exchanged by metal ions, the contents of both Na and Mg further decreased sharply. After ion exchange, the molar ratio of metal to Mn is in the range of 0.06−0.27, as obtained from ICP-AES analyses (bulk ratio). These bulk ratios are considerably larger than those given by EDX data (surface ratio), which are less than 0.1. These data suggest that the introduced metal is in the layers instead of decorating the outside surface of particles. The basal *d* spacings (001 reflection) of metal−buserites vary with different metal species in the range of 9.3−11.2 Å. The corresponding *c*

---

(38) Tian, Z.; Yin, Y.; Suib, S. L.; O'Young, C. L. *Chem. Mater.* **1997**, *9*, 1126−1133.

(39) Post, J. E.; Von Dreele, R. B.; Buseck, P. R. *Acta Crystallogr.* **1982**, *B38*, 1056−1064.

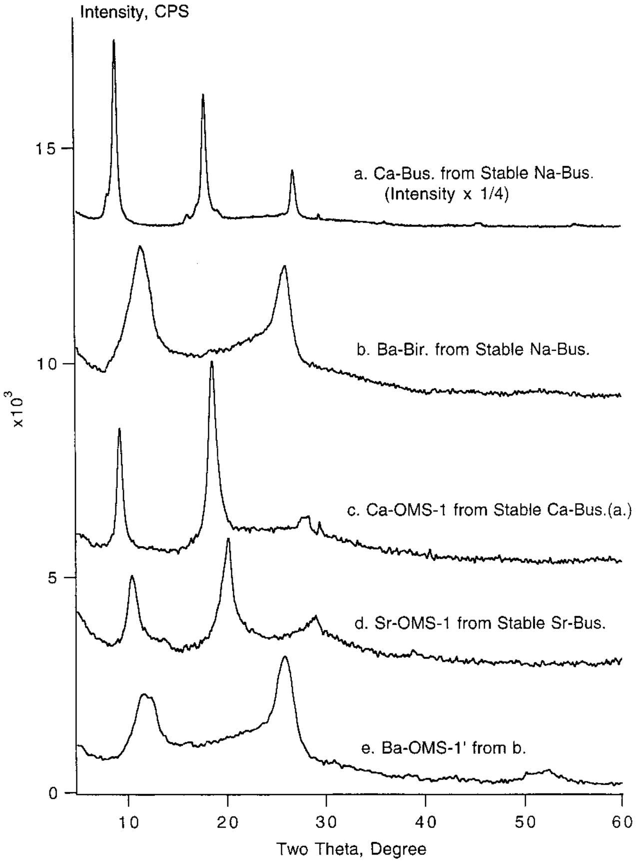

Figure 9. XRD patterns of buserites from ion exchange of stabilized Na−buserite with group II elements and corresponding autoclaved products (150 °C for 2 days).

dimensions therefore change in the range 9.3−11.2 Å with the introduction of different metal ions.

The metal loading introduced during exchange usually increased with increasing the concentration of metal ions as well as with time until equilibrium is achieved, both at the cost of the contents of Na and Mg. A repeated exchange can also considerably increase the metal content. However, the metal loading content considerably decreased when the exchange was done over 65 °C. This is consistent with our previous work that higher temperatures (> 65 °C) can fix exchangeable ions in birnessite. The content of a specific metal ion should also depend on the relative capability in competitive exchange among metal species such as Na^+ and Mg^{2+}.

Discussion

A. Physicochemical Changes during Stabilization of Na−Buserite by Aging in DDW. A stabilized Na−buserite is different from unstable Na−birnessite and a Mg−buserite in composition (type and amount of interlayer ions, amount and uniformity of interlayer hydrates), thermal stability, and ion-exchange properties. AES and EDX studies show that stabilized Na−buserite has less Na^+ content than Na−birnessite. IR studies indicate no structural changes in the framework during stabilization or ion exchange, but the uniformity of hydrates and therefore the ordering of layers are improved. SEM indicates that Na−buserite keeps its morphology during the stabilization process, during ion exchange with Mg^{2+}, and during subsequent hydrothermal treatment to Mg−todorokite. TGA/DSC show that the thermal stability of the framework exhibits almost no difference but the capability of interlayer ions to retain the interlayer hydrates is improved. CO_2-TPD shows that the density of basic sites is reduced upon a second aging but the strengths of the basic sites are similar. Above all, the number of metals incorporated into stable buserites which are subsequently converted into todorokites is greatly increased.

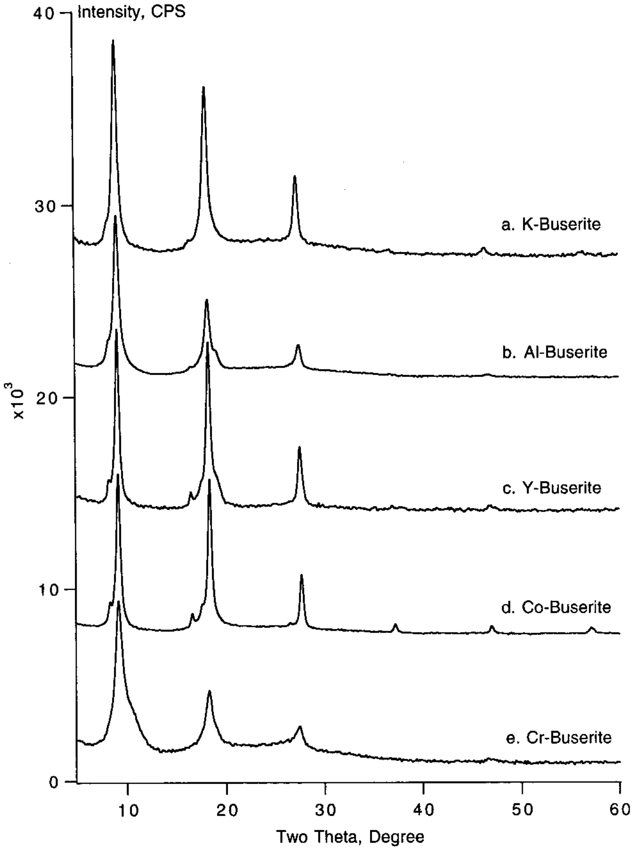

Figure 10. XRD patterns of several metal−buserites from ion exchange of stabilized Na−buserite.

The stability of buserite or birnessite is determined by the capability of the interlayer ion to control its surrounding water molecules. For example, in the case of ion exchange of unstable Na−buserite with alkaline earth metals, Mg^{2+} has the highest charge/radius ratio among the ions and therefore has the largest capability of retaining water molecules. This results in a stable buserite with double interlayer hydrates. Meanwhile, Sr^{2+} and Ba^{2+} in birnessites without a second aging are only capable of retaining monolayer hydrates.

The synthesis of Na−buserite is done in highly basic media. Some of the NaOH used can be included between the layers of buserite. It is very hard to wash this off during a short time washing. After a Na−buserite sample was washed until the pH of the filtrate solution was below 10, it was stirred in DDW for a few hours. The pH of the supernatant solution was found to be over 12. When washed Na−buserite is stirred in DDW for 2 days (the second aging), there is enough time for extra NaOH species included in Na−buserite to diffuse out, leading to a product which is virtually neutral between the layers.

One of the consequences of the presence of extra NaOH is that the interlayer cation's capability of retaining the surrounding hydrates will be diminished. The hydrates in Na−buserite are retained by the electrostatic force of Na^+ ions. A nearby OH^- ion can interact with a Na^+ ion, shielding a part of its positive charge and repelling the negative ends of surrounding water molecules. The power of Na^+ ions to attract the surrounding water molecules is therefore reduced due to the presence of OH^- ions. After a second aging, the interlayer Na^+ ions can interact

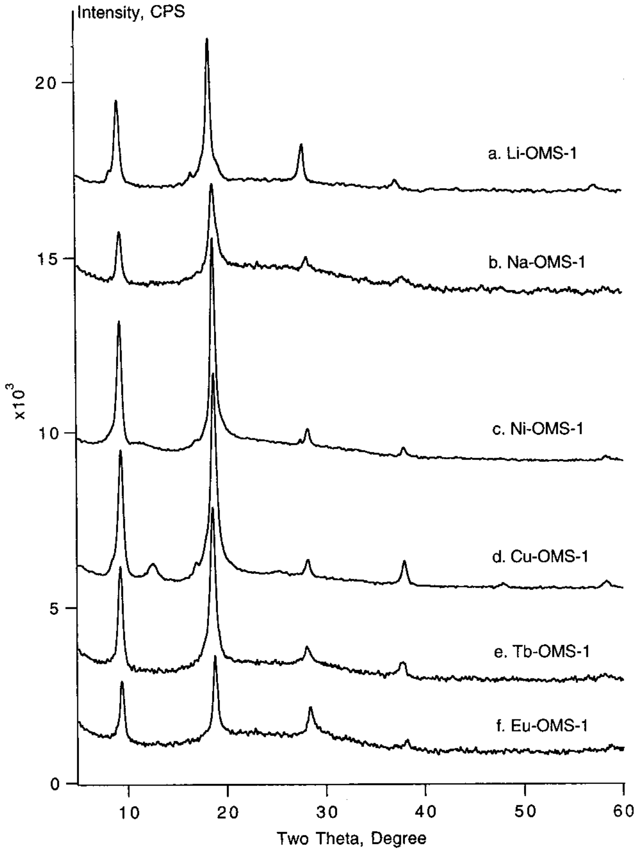

Figure 11. XRD patterns of various metal−todorokites from autoclaving metal−buserites based on stabilized Na−buserite (140−150 °C for 40−48 h). Higher temperatures for a longer time may lead to formation of some manganite, γ-MnOOH.

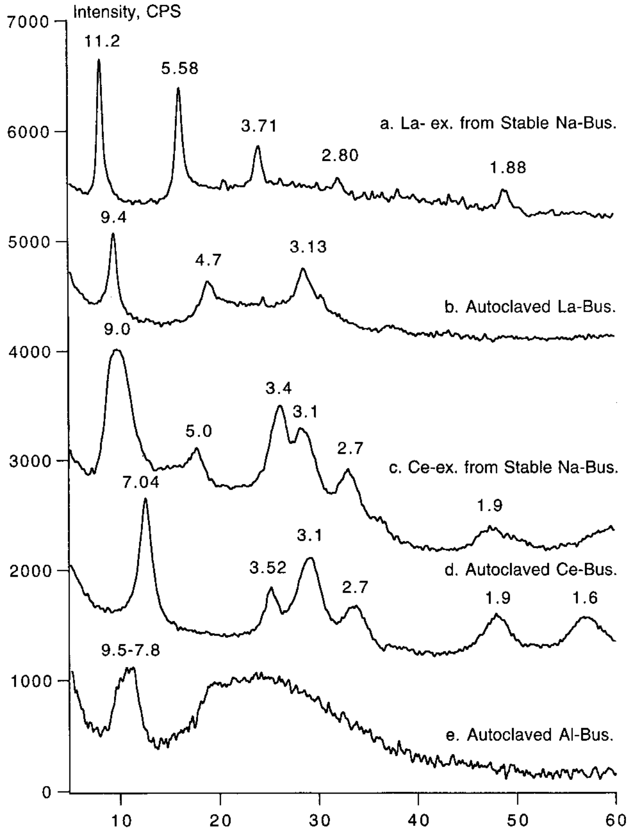

Figure 12. XRD patterns of some stable or unstable buserites (from ion exchange of stabilized Na−buserites) and Corresponding Autoclaved Products (140−150 °C for 40−48 h). Figures over XRD peaks are *d* spacings in Å.

strongly with surrounding water molecules in contrast to an unstabilized Na−buserite.

Another effect may also arise from the second aging treatment which makes the interlayer microenvironment less basic. Several authors studied the stability enhancement effect of Mg^{2+} added initially in the gelation stage.[17,36,38] The magnesium species may be partially situated between the layers of buserite in the form of $Mg(OH)_2$ in this highly basic system. When the bulk of the buserite becomes less basic, $Mg(OH)_2$ may slightly ionize to produce some interlayer Mg^{2+} ions, which may interact more strongly with interlayer water molecules. Na−buserite prepared by double aging is thus stabilized. The sharp decrease of Mg content of stabilized buserites during exchange with metal ions confirms that large portions of Mg^{2+} ions are exchanged after stabilization. This may also increase the number and amount of metal ions which can be introduced into stabilized Na−buserite by ion exchange.

CV studies of Figure 7 indicate the disproportionation of Mn^{3+} into Mn^{4+} and Mn^{2+}, in agreement with the increase in average oxidation state of manganese for many metal-exchange buserites. The reduced Mn^{2+} can enter the solution or the layers to act as anchors for hydrated species, which, together with hydrated Mg^{2+}, stabilize double-aged buserites.

B. Application of the Double-Aging Method in the Transformation of Buserite (Layered Structure) into Todorokites (Tunnel Structure) Incorporated with Various Metals. The immediate application of the double-aging method is to prepare todorokites with various metals, which is an important goal for many studies since they are important catalysts for many reactions. Although many metals have been found in manganese nodules where birnessite and todorokite are the main manganese oxide phases, only a limited number of metals have been incorporated into todorokite, such as Mg, Ni, Co, Cu, Mn, and Zn.

Discussions above show that differences in stability of layered buserite can lead to differences in phases of the corresponding products (OMS-1 or OMS-1′) during hydrothermal treatment. OMS-1 is produced from Mg−buserite or a few other metal−buserites by hydrothermal treatment. The mechanism for this transformation is not yet clear. In this work, many other metal−buserites, such as Li−buserite and Ca−buserite, can form either OMS-1 or OMS-1′, depending on whether a double-aging treatment is done. The formation of OMS-1 and OMS-1′ is correlated with interlayer ions and the corresponding capability of controlling hydration.

The ability of an interlayer ion in buserite to control the surrounding water molecules decreases with increasing temperature. This is similar to the fact that the diameter of an aqueous ion decreases with increasing temperature. For a metal−buserite in an aqueous environment, an increase in temperature can lead to a decrease in the *d* spacing of the basal XRD reflection, which is mainly determined by the number of interlayer water molecules. When a double-aged Li−buserite is directly hydrothermally treated (150 °C, 2 days), a Li−todorokite can be obtained. Li−buserite from ion-exchange of stable Na−buserite is a stable buserite, even retaining the buserite structure after sitting in DDW at 90 °C for 3 days. It gradually converts to a Li−birnessite after being in DDW at 90 °C for 7 days. The same hydrothermal treatment of a converted Li−birnessite only produces an OMS-1′ type phase.

A Ca− or Sr−buserite from stabilized Na−buserite keeps the buserite structure even when it is autoclaved at 150 °C for

Table 1. Compositional Data for Na—Birnessite, Stabilized Na—Buserite, Metal—Buserites, and Metal—Todorokites, As Determined by ICP-AES,[a] TGA, and Average Oxidation State of Mn

Sample	composition	av oxidn state of Mn[a]
Na—Birnessite	$K_{0.005}{\cdot}Na_{0.39}{\cdot}Mg_{0.042}{\cdot}0.044MgO{\cdot}MnO_{1.76}{\cdot}0.77H_2O$	3.52
Na—buserite	$Na_{0.26}{\cdot}Mg_{0.055}0.016MgO{\cdot}MnO_{1.81}{\cdot}1.16H_2O$	3.63
K—buserite	$K_{0.24}{\cdot}Na_{0.038}{\cdot}Mg_{0.035}{\cdot}0.012MgO{\cdot}MnO_{1.83}{\cdot}0.78H_2O$	3.65
Mg—buserite	$Na_{0.024}{\cdot}Mg_{0.17}{\cdot}0.07MgO{\cdot}MnO_{1.82}{\cdot}1.19H_2O$	3.64
Cu—buserite	$Na_{0.012}{\cdot}Cu_{0.065}{\cdot}Mg_{0.045}0.023MgO{\cdot}MnO_{1.89}{\cdot}0.78H_2O$	3.77
Ni—buserite	$Na_{0.022}{\cdot}Ni_{0.11}{\cdot}Mg_{0.03}{\cdot}0.024MgO{\cdot}MnO_{1.86}{\cdot}0.83H_2O$	3.71
Ce—buserite	$0.009Na_2O{\cdot}0.063MgO{\cdot}0.035CeO{\cdot}MnO_{1.76}{\cdot}1.18H_2O$[c]	
Eu—buserite	$0.010Na_2O{\cdot}0.061MgO{\cdot}0.028EuO{\cdot}MnO_{1.84}{\cdot}1.22H_2O$[c]	
Mg—OMS-1	$Na_{0.014}{\cdot}Mg_{0.24}{\cdot}0.051MgO{\cdot}MnO_{1.78}{\cdot}0.92H_2O$	3.55
Cu—OMS-1	$Na_{0.015}{\cdot}Cu_{0.09}{\cdot}Mg_{0.050}{\cdot}MnO_{1.84}{\cdot}0.75H_2O$	3.68
Ni—OMS-1	$Na_{0.018}{\cdot}Ni_{0.13}{\cdot}Mg_{0.038}{\cdot}MnO_{1.81}{\cdot}0.73H_2O$[d]	3.60

[a] Relative errors of elemental analyses are ca. 5%. [b] See ref 17 for detail. In MnO_x, x is determined from the average oxidation state. The formulas are calculated from ICP-AES and TGA data. Mg contents more than necessary for charge compensation are given in the forms of oxides. [c] Only metal/water contents are available. The balance results in total oxygen contents. [d] Total ions are not enough for charge balance, possibly due to analysis errors.

30 min and is converted to Ca— or Sr—todorokite after hydrothermal treatment. Under the same conditions a Ca— or Sr—buserite produced from ion exchange of an unstable Na—buserite changes to a birnessite structure after it is heated at 150 °C for 30 min, forming an OMS-1′ structure after hydrothermal treatment for 2 d. This result indicates that only stable buserite can interact strongly with interlayer ions to retain the double-layer hydrates in the buserite structure at elevated temperatures (for a short time). This material gradually converts to todorokite (having a tunnel structure) during the hydrothermal treatment. Unstable buserites and a few stable buserites will change to birnessite at elevated temperature, giving rise to OMS-1′.

A Mg—buserite, irrespective of double aging or not, can keep the buserite structure at elevated temperatures (90 °C for 7 d) and even at 150 °C for 2 h. Further hydrothermal treatment results in a change in the relative intensity of XRD reflections of 4.86 and 9.7 Å, which may suggest a gradual transformation from buserite to todorokite. Only layered MnO_x materials which can retain the buserite structure for some time (e.g., >30 min) under hydrothermal conditions can be converted to OMS-1. Some more direct techniques such as high-resolution electronic microscopy are required for detailed description of the transformation process.

C. Interconversion among Buserite, Birnessite, Dehydrated Birnessite, and Other MnO_x Phases. Buserite, birnessite, and dehydrated birnessite are linked by variation in the randomness of hydrates. There appear to be continuous intermediates between buserite and birnessite as well as between birnessite and dehydrated birnessite, differing in the distance of the MnO_6 sheets. A scheme illustrating these phase transformations is given in Figure 1, where feitknechtite, a layered material with an interlayer distance of 4.7 Å, is a precursor to buserite or birnessite.[27]

As suggested by Turner et al. and Golden et al.,[6,11] birnessite and buserite are the sheet structure end-members of the hollandite—romanechite and todorokite series, respectively. This is in accordance with the observation in this study that a buserite which is stable under hydrothermal conditions for some time transforms to the todorokite (OMS-1) structure while an unstable buserite (birnessite) is converted to an OMS-1′ phase. This OMS-1′ could be a tunnel MnO_x material similar to the hollandite—romanechite structure (see Figure 13).

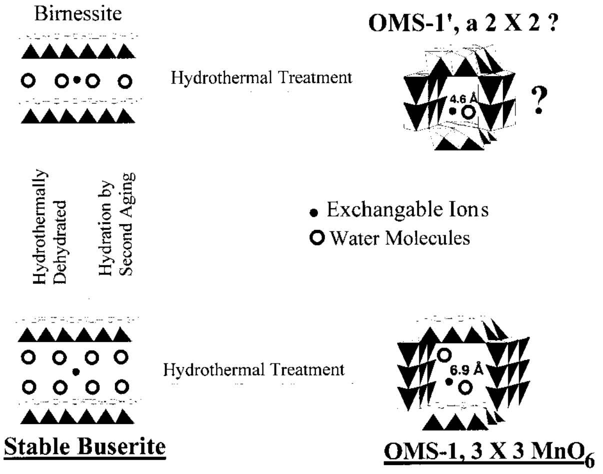

Figure 13. Illustration of transformation of layered structure to tunnel manganese oxide, showing that only stable buserites can be hydrothermally converted to a todorokite-type tunnel structure.

The basal *d* spacing of a newly dried La—buserite is 11.2 Å (Figure 12a), larger than those of normal buserites (<10 Å). This basal *d* spacing gradually shifts to 10 Å when the sample is sitting in air for ca. 30 min. The 11.2-Å *d* spacing may correspond to triple interlayer hydrates between adjacent sheets of La—buserite. When some large organic ammonium ions are incorporated into the MnO_6 sheets, buserite-type MnO_x materials with various large *d* spacings are produced.[10,11,28] Attempts to synthesize tunnel structure MnO_x with larger tunnel size than todorokite from these larger *d* spacing layered MnO_x materials are under way.

Conclusions

A stabilization procedure of aging an as-synthesized Na—buserite in DDW leads to the production of stable Na—buserite, which is stable in air at room temperature. Over 25 kinds of ions have been ion-exchanged into this stabilized Na—buserite, forming various stable metal—buserites, including group I/II metals and some other main-group metals, transition metals, and lanthanides. Todorokite type manganese oxides (OMS-1) incorporated with these metals have been produced by hydrothermal treatment of these materials. Only stable buserites can be hydrothermally converted to todorokites. Hydrothermal treatment of unstable metal—buserites leads to the production of OMS-1′, probably an alternative hollandite.

Acknowledgment. The authors acknowledge the support of the Office of Basic Energy Sciences, Division of Chemical Sciences, of the Department of Energy. We are also grateful to Dr. F. S. Galasso for helpful suggestions and discussions.

IC980675R